CHEMISTRY
A EUROPEAN JOURNAL

DOI: 10.1002/chem.200700504

The Reactivity of Calicheamicin γ_1^I in the Minor Groove of DNA: The Decisive Role of the Environment

Elfi Kraka,*[a] Tell Tuttle,[b] and Dieter Cremer[a]

Abstract: Triggering and Bergman cyclization of calicheamicin γ_1^I outside and inside the minor groove of the duplex 9mer-B-DNA sequence d(CACTCCTGG)·d(CCAGGAGTG) were investigated by using density functional theory and molecular mechanics (DFT and MM) descriptions in which the ligand is completely described at the DFT and the receptor at the MM level. The calculated docking energy of calicheamicin γ_1^I (-12.5 kcal mol^{-1}) is close to the measured value of -9.7 kcal mol^{-1} and the site specificity is in line with experimental observations. Calicheamicin is triggered in the minor groove in such a way that out of a cyclohexenone by Michael addition an *E* rather than a *Z* form of a cyclohexanone is formed, which in turn adopts a chair rather than a twistboat form. Decisive for the stereochemistry of the Michael addition is the orientation of the carbamate substituent at the headgroup of calicheamicin. Triggered calicheamicin can undergo the Bergman cyclization at body temperature only if present in its E chair form (activation enthalpy 16.4 kcal mol^{-1}). An intermediate biradical is formed (docking energy -13.6 kcal mol^{-1}), which has a sufficient lifetime to abstract two hydrogen atoms. Hydrogen abstraction is a two- rather than one-step process and involves the C5(H5′) atom first and then the T22(H4′) atom in line with experimental observations. The decisive role of using a DFT rather than an MM description for the ligand is documented.

Keywords: ab initio calculations · calicheamicin · DNA damage · environmental effects · reaction mechanisms

Introduction

The discovery and recognition of the astonishingly selective activity of the naturally occurring enediynes has generated intense chemical, biological, and medicinal interest in these remarkable compounds.[1–4] The naturally occurring enediynes are a family of secondary metabolites that include neocarzinostatin, esperamicin, dynemicin, kedarcidin, and the target compound of this work, (−)-calicheamicin γ_1^I (**1**, Scheme 1).

[a] Prof. Dr. E. Kraka, Prof. Dr. D. Cremer
Department of Chemistry and Department of Physics
University of the Pacific
3601 Pacific Avenue, Stockton, CA 95211–0110 (USA)
Fax: (+1) 194-62-607
E-mail: ekraka@pacific.edu

[b] Dr. T. Tuttle
Department of Pure and Applied Chemistry
University of Strathclyde
295 Cathedral Street
Glasgow, G1 1XL (UK)

Supporting information for this article is available on the WWW under http://www.chemeurj.org/ or from the author.

Enediyne **1** comprises the aglycone calicheamicinone (see also Scheme 2, Model 4) and the sugar tail with rings A, B, C, D, and E. Discovered in 1986 as a fermentation-derived antitumor antibiotic that is produced by *Micromonospora echinospora* (subspecies calichensis),[4] it possesses excellent potency against murine tumors P388,[4] L1210 leukemias, and solid neoplasms such as colon 26 and B16 melanoma.[4,5]

The structure of **1** was determined in a stepwise approach that included the X-ray diffraction analysis of rings B and C as a single isolated unit,[6] extensive NMR studies of ring A and its attachment to ring B, ring D, and its connection to C,[5] as well as the isolated ring E.[7] The structure and attachment of the aglycone was established through a combination of NOE experiments and X-ray crystallography on derivatives.[6] The original stereochemistry, which was proposed for the aglycone at the position of the attachment to ring A, was later revised on the basis of the structure of esperamicin. The revised stereochemistry places the glycosidic linkage to ring A on the same side of the enediyne plane as the methyl trisulfide,[8] thus leading to *S* and *R* absolute configurations at the stereogenic centers C1 and C8.

The configuration of native **1** was later confirmed by the enantioselective total synthesis of (−)- or (*S*,*R*)-calicheami-

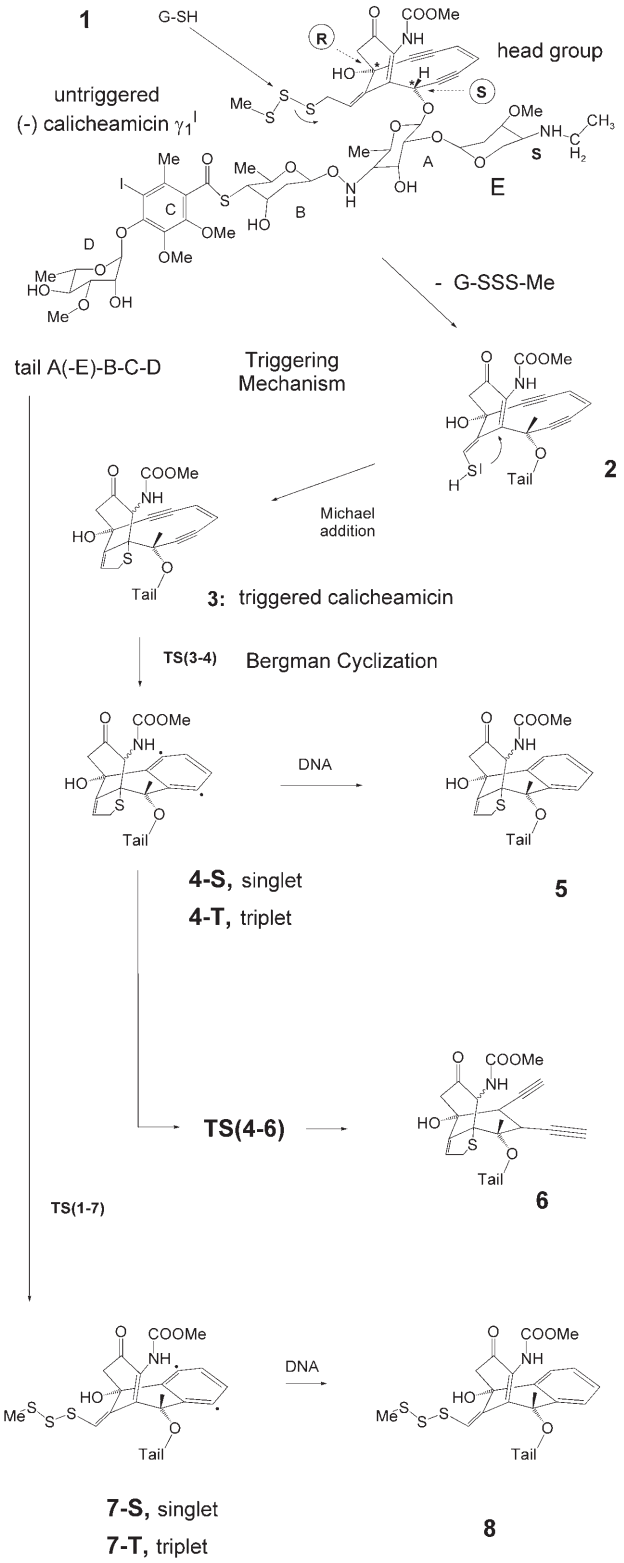

Scheme 1.

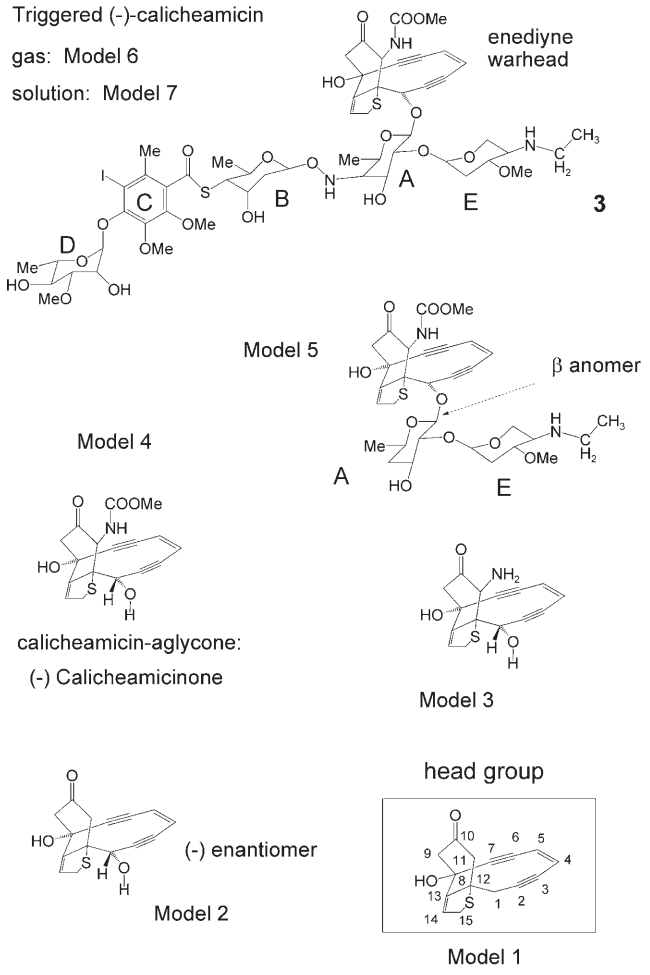

Scheme 2.

cone[9] and (−)- or (*S*,*R*)-**1** in their enantiomerically pure form.[10] Syntheses of (−)-calicheamicinone through different synthetic routes have also been successfully undertaken,[11,12] and in the course of the synthetic work an X-ray diffraction analysis of the aglycone could be performed. The crystal structure is observed to have a relatively planar (slightly deformed to a twistchair) cyclohexenone ring and the carbamate group is oriented in such a way that it runs parallel to the enediyne warhead (i.e., opposite to the sulfur moiety).

In its native form, **1** is inactive, only once it is triggered does it become active. The triggering involves a nucleophilic attack at the trisulfide linkage[3,4] leading to the thiol **2** (Scheme 1), which can undergo an intramolecular Michael addition to form the triggered calicheamicin **3**, characterized by its tricyclic headgroup. Once triggered the molecule undergoes a Bergman cyclization[13,14] via **TS(3–4)** to form the singlet biradical **4-S**, which, if properly positioned in the minor groove, subsequently abstracts two hydrogen atoms from the DNA strands to form the stable benzene derivative **5**. Alternatively, **4-S** can undergo a retro-Bergman reaction via **TS(4–6)** yielding the open enediyne **6** (Scheme 1).

Hydrogen abstraction by **4-S** leads to oxidative double-strand scission, which causes irreversible damage and cell death (apoptosis).[1–4,15,16] This was first demonstrated by Zein and co-workers[17] through the ability of **1** to cause in vitro double-strand scission when in the presence of thiols.

Furthermore, the sequence specificity of the cut site of **1** was found to be well defined.[17] Chemical footprinting studies established the binding site for calicheamicin as oligopurine•oligopyrimidine tetranucleotide stretches, with the highest specificity being identified as the (T-C-C-T)•(A-G-G-A) sequence.[17–19] It was also demonstrated that **1** abstracts hydrogen atoms from DNA rather than from the surrounding medium (proteins, etc.) and that the carbon sites that extract the DNA hydrogens are exactly the proradical carbons involved in the Bergman cyclization.[20]

There have been numerous studies clarifying the site specificity of hydrogen abstraction,[21–23] its dependence on the oligosaccharide tail,[16,24–27] the interactions of the tail with DNA, and their mutual repositioning.[28,29] These studies were extensively based on NMR measurements, which in turn laid the basis for molecular modeling descriptions.[30,31] So far, only a few quantum chemical studies have been carried out to investigate the triggering of the aglycone (model 4 in Scheme 2),[32] the stereochemistry of its Michael addition,[33] or the Bergman cyclization of the headgroup.[34] A full quantum chemical investigation of **1** or **3** utilizing either density functional theory (DFT) or wave function theory has so far not been carried out.

In this work, we present a DFT and molecular mechanics (MM) investigation in which the ligand (**1**, **3** or their follow-up products) is for the first time completely described at the DFT level and the receptor by MM. We investigate the energetics and stereochemistry of the triggering and the Bergman reaction in dependence of the substituents sitting at the headgroup. For the latter purpose, we stepwise simplify the triggered molecule **3** to obtain the models 1 to 7 shown in Scheme 2. Normally, it is assumed that the headgroup determines the energetics of the Bergman reaction. We explicitly test this claim and determine the best model for explaining the biological activity of **3** as accurately as possible.

This investigation also focuses on the docking of **3** in the minor groove of DNA. Docking simulations reveal the specificity of the docking process and its importance for the activity of **3**. This work is part of a general project aimed at designing nontoxic enediyne-based antitumor drugs. The project comprises four steps: 1) investigation of simple enediynes to understand the sensitivity of the Bergman reaction on substituents and environmental effects;[35–40] 2) investigation of docking, triggering, and biological activity of natural enediynes;[41,42] 3) design of a new enediyne warhead that will better fulfil (relative to toxic natural enediynes) the requirements of a potent antitumor drug;[39,40,43] 4) design of a new class of antitumor drugs. The present work pursues the second goal of this general project.

Computational Methods and Strategies

The description of **1** docked into the minor groove of DNA would be best done by a quantum mechanics (QM)/MM approach, provided sampling into the μs range would be possible, which is the typical timescale for ligand binding (dissociation) to (from) DNA. This, however, exceeds the possibilities of modern QM/MM molecular dynamics (MD) simulations. Alternatively, one could attempt to describe the ligand and receptor exclusively by MM. This implies setting up a suitable force field that is able to describe the enediyne unit and the chemical processes of this unit along the Bergman cyclization path while bound to DNA. Such a force field, however, is hampered by the principal problem of describing quantitatively quantum-mechanical processes with empirical force fields. Because these basic questions have not been solved and will not be solved in the near future one has to revert to a simplified solution. In this work we extensively used DFT to describe ligand **1** as accurately as possible. Once the configuration of the ligand **1** was determined it was kept during the docking to the receptor DNA. The latter was described at the MM level and the docking process was described with the help of empirical scoring functions that were parameterized to get useful complex free binding energies in the case of proteins. In this way, we obtained a rigid docking description of a QM+MM (rather than a QM/MM) description, the usefulness of which was described in previous work.[42]

Based on previous work[40–43] and according to the arguments given in the Supporting Information, we used DFT with Pople's 6–31G(d)[44] and 3–21G split-valence basis sets[45] in connection with the hybrid functional B3LYP[46–48] to describe **1**. (For calculations with larger basis sets such as 6–31G(d,p), 6–31+G(d), 6–311G(d,p), and 6–311++G-(3df,3pd) and the use of CCSD(T), see Supporting Information.) At B3LYP/3–21G, the geometries of **1**, **3** and all follow-up products were fully optimized. Restricted DFT (RDFT) calculations were carried out for the singlet states, however, in each case the internal and external stability of the RDFT solution was tested.[49] If the latter was not fulfilled as, for example, in the case of the singlet biradical **4-S** (Scheme 1), a broken-symmetry unrestricted DFT (BS-UDFT) calculation was performed for the singlet state. The triplet states investigated in this work were calculated at the UDFT level of theory. Frequency calculations were performed for models 1 to 4 (Scheme 2) to obtain activation enthalpies $\Delta H(298)^a$, reaction enthalpies $\Delta H(298)_R$, and singlet–triplet splittings ΔH(S–T) at 298 K. In addition, entropies S(298) and free energies $\Delta G^a(298)$ or $\Delta G_R(298)$ were calculated. Frequency calculations were also used to ensure the attainment of the correct transition state, as witnessed by a single imaginary frequency corresponding to bond formation. In addition, intrinsic reaction coordinate (IRC) calculations were carried out for models 1 to 5 to clarify that the mode being followed belongs to the Bergman cyclization. Solvent effects were determined by employing the static isodensity surface polarized continuum model (IPCM).[50] For all quantum chemical calculations, the program packages COLOGNE2006[51] and Gaussian98[52] were used.

Conformational changes of the cyclohexanone ring of the headgroup of **1** were determined with the help of the Cremer–Pople puckering coordinates (puckering amplitudes

$q2$ and $q3$ and pseudorotational phase angle ϕ_2; alternatively total puckering amplitude Q and polar angle $\Theta = \arctan\{q2/q3\}$).[53,54] Throughout the text, ideal conformational forms such as chair (C), twistboat (TB), or boat (B) of cyclohexanone will be distinguished from distorted C, TB, or B forms by indicating both ideal and real ϕ_2 values in the case of the B-TB family, or both ideal and real Θ values in the case of the C forms leading to notations such as TB{30, 39} (9° deviation from ideal TB) or C{180, 176} (4° distortion in the direction of the ideal B-TB family at $\Theta = 90°$). This notation is simplified to **TB30**, **B60**, **TB90**, etc. in the case of ideal forms, which have to be specified with regard to their ϕ_2 value. The conformational globes presented in the Supporting Information facilitate the reading of this notation.

Docking studies were carried out for the full gas-phase optimized geometries. The receptor used in these studies was modeled by a duplex 9mer-B-DNA sequence d(CACTCCTGG)·d(CCAGGAGTG), from which the original starting geometry was taken (PDB ID: 2PIK).[31] This geometry had been previously minimized with the embedded form of **1** by using MM, MD, and the distance constraints arising from the NOE data for the complex.[31] The docking procedure was carried out by using AutoDock version 3.0.5.[55] The orientation of the docked structure of **1** and the subsequent reaction species in the minor groove of DNA are presented by plotting the Connolly surface[56] of DNA and the capped-stick representation of the ligand. Receptor–ligand interactions were analyzed by using the electrostatic potential (EP), which was mapped onto the Connolly surface.

Results and Discussion

Results are presented in the following way. In the first two sections, we discuss the stereochemistry of the triggering reaction and the energetics of the Bergman cyclization, considering in the latter case different stereochemical results of the Michael addition. The tail structure is investigated in the third section. The fourth section is devoted to a discussion of the docking of **1** and its follow-up products in the minor groove of DNA. In the fifth and final section, the triggering of **1** is reinvestigated considering the situation in the minor groove.

Triggering of calicheamicin: energetics and stereochemistry: One could speculate that the enediyne system of untriggered **1** can undergo Bergman cyclization via **TS(1–7)** to biradical **7**, which then abstracts hydrogen atoms from DNA to stabilize as benzene derivative **8** (Scheme 1). According to B3LYP calculations, a Bergman cyclization of **1** requires at least 48.0 kcal mol^{-1} activation energy ($\Delta H^{\ddagger} = 46.4$ kcal mol^{-1}), which is far too high to be of any relevance at body temperature. Hence, **1** has to be converted via **2** to **3** to undergo Bergman cyclization at normal temperature. Formally, this conversion can be described by Equation (1):

$$\mathbf{1} + \text{Me}-\text{SH} \rightarrow \mathbf{3} + \text{Me}-\text{S}-\text{S}-\text{S}-\text{Me} \quad (1)$$

in which thiol Me–SH represents gluthathione. This reaction (R1) is exothermic by 36.8 kcal mol^{-1} (B3LYP/3–21G). Some of this energy should result from the exchange of an SH and C=C double bond against a S–C, C–H, and C–C single bond (estimated gain of 14 kcal mol^{-1} when experimental bond-dissociation enthalpies are used[57]). The larger part, however (22 kcal mol^{-1}) should result from changes in the strain energy of the calicheamicin aglycone in which both the conversion of a cyclohexenone to a cyclohexanone ring and the strain relief in the enediyne unit play a role.

The key for the understanding of the strain factors determining the Bergman cyclization barriers for **1** and **3** is the fact that the formation of the *p*-benzyne biradical implies also the formation of an annelated cyclohexene ring, which prefers a half-chair conformation (puckering coordinates: $Q(\text{total}) = 0.457$, $q3 = 0.277$ $q2 = 0.364$ Å, $\Theta = 127.3$ $\phi_2 = 30°$,[58] see cyclohexene globe in the Supporting Information) with the largest pucker at the bridge bond C12–C13 (see model 1 in Scheme 2) carrying the external double bond. This becomes possible when the adjacent cyclohexanone ring converts into a C or TB form (see Supporting Information). In **1**, the cyclohexenone ring is frozen in a half-chair form itself so that a large strain energy builds up in the TS of the Bergman reaction raising the reaction barrier to 48 kcal mol^{-1}.

The Michael addition, which is part of the triggering mechanism, has the task to convert the cyclohexenone ring into a cyclohexanone ring and, thus, improve the ring-strain situation by about 30 kcal mol^{-1}. In connection with the Michael addition, one has to consider that the nucleophilic SH group in **2** (Scheme 1) can only attack the internal double bond of the cyclohexenone ring from above (Scheme 1). There is, however, the possibility that the carbamate group is either positioned *Z* or E with regard to the newly formed dihydrothiophene ring (indicated in Scheme 1 by a wiggled C–N bond). Apart from this, each isomer can adopt a number of conformers, which may be decisive for the barrier of the Bergman cyclization: If a conformer is formed that is destabilized by strain effects, the barrier will most likely be reduced because this strain is felt less in the TS of the Bergman cyclization (formation of a benzene ring), provided the cyclohexanone ring can adopt a conformation that accommodates the dihydrothiophene ring in **3**. The opposite is true for a particularly stable *Z* or E form of the enediyne. This is a well-known principle for manipulating the reactivity of an enediyne (strain principle),[35,59] which also plays an important role for **3**, as we see in the following.

Conformational behavior of the cyclohexanone ring: For the purpose of predicting the most stable isomer and conformer resulting from the Michael addition, we investigated the conformational behavior of cyclohexanone (for details, see Supporting Information). Cyclohexanone prefers a chair form that is 4.2 kcal mol^{-1} more stable than the twistboat form TB30. Annelation of the dihydrothiohpene ring increases the C-TB energy difference to 5.6 kcal mol^{-1}. If carbamate and OH groups are added *Z* and E forms are distinguished and in the case of the E form the C-TB energy dif-

ference increases to 10 kcal mol^{-1}. For the *Z* forms, C and TB become comparable in energy (0.4 kcal mol^{-1} in favor of C) because the latter form benefits from electrostatic attraction and hydrogen bonding between the carbamate and the neighboring keto group.

When combining the influence of the annelated dihydrothiophene ring, the carbamate group, and the enediyne bridge as in model 4 (Scheme 2), form **3-Z-TB**{30, 44} gains stability because of a stronger pucker of this form (see Supporting Information) and a suitable (more outward) orientation of the bonds connecting the enediyne bridge to the cyclohexanone ring leads to a less-strained system than in the case of form **3-E-C**{180, 156}. Accordingly, **3-Z-TB**{30, 44} is most stable, followed by **3-E-C**{180, 156} ($\Delta E =$ 1.9 kcal mol^{-1}, see Supporting Information), the **3-Z-C**{180, 159} ($\Delta E = 7.6$ kcal mol^{-1}), and the **3-E-TB**{30, 41} form ($\Delta E = 10.7$ kcal mol^{-1}). Hence, from the multitude of possible conformers, only two, **3-Z-TB**{30, 44} and **3-E-C**{180, 156} remain, and these are stabilized by a compromise of internal angle widening at the sp^2-hybridized C atoms, staggering of external bonds, intramolecular hydrogen bonding, accommodation of the annelated dihydrothiophene ring, and minimization of the strain in the enediyne unit.

We note in this context that the keto group is oriented in the C forms toward and in the TB forms away from the enediyne bridge, which might indicate that the C and TB forms result from two different stereochemical situations of the Michael addition leading to *E* or *Z* configurations. This question is discussed in more detail below.

Typical of the Michael addition is that an enolate is formed, which is protonated at the negatively charged oxygen atom. Rearrangement of the enol to a keto form leads to the triggered calicheamicin **3** (Scheme 1). Because 1) the proton stems most likely from a solvent molecule rather than the SH group and 2) the enol is most likely a real intermediate with a finite lifetime, the tautomerization of the enol to the ketone **3**, which is known to be catalyzed by water molecule(s),[60] can lead to *Z* or *E* configuration. If one does not consider a possible role of DNA in supporting the formation of either the *Z* or *E* isomer, the only way of making any prediction is to assume thermodynamic control, which suggests that a large amount of **Z-TB** is formed beside a relatively small amount of **E-C**. In any case, however, there should not be any **Z-C** or **E-TB** conformers in the reaction mixture.

Because factors such as solvent and complexation of **3** to DNA may increase the amount of **E-C**, we do not focus exclusively in the following on the **Z-TB** isomer, but consider also the possibility that the **E-C** isomer of **3** plays a role. Next, we investigated which of the two isomers should be biologically more active.

Energetics of the Bergman cyclization: In Tables 1 and 2, the calculated energetics for the Bergman cyclization of **3-Z-TB**{30, 44} and **3-E-C**{180, 156} are summarized. There is little change in the relative energies in dependence of the model chosen. For **3-Z-TB**{30, 44} (Table 1), the activation enthalpy $\Delta H^a(298)$ varies between 25 and 31 kcal mol^{-1} with

Table 1. Energetics for the Bergman cyclization reaction of the *Z*-twistboat (Z-TB) conformation of (−)-calicheamicin γ_1^I (**1**).[a]

Model	Structure	E, ΔE	ZPE	H, ΔH	S	G, ΔG	μ	imag. ω
1	**3**	−1121.31829	144.0	−1121.072321	122.4	−1121.13050	4.51	
	TS(3–4)	27.4	142.5	25.5	120.7	26.0	3.64	
	4-S	5.9	144.3	5.5	118.6	6.6	4.31	440*i*
	4-T	2.4	144.5	2.6	120.9	2.0	4.32	
2	**3**	−1196.10777	146.3	−1195.857149	126.2	−1195.91710	4.99	
	TS(3–4)	27.2;*24.1*	144.8	25.2;*22.1*	124.5	25.7	4.40	
	4-S	6.7	146.2	6.1	124.3	6.7	4.25	433*i*
	4-T	2.5	146.6	2.6	126.6	1.9	4.27	
3	**3**	−1251.14965	156.7	−1250.88119	131.5	−1250.94366	4.89	
	TS(3–4S)	28.3;*25.1*	155.0	26.3;*23.1*	129.8	26.8;*23.6*	4.37	
	4-S	8.4	156.6	7.9	129.4	8.5	3.99	432*i*
	4-T	2.5	156.9	2.8	131.7	2.1	4.01	
4	**3**	−1477.78955	183.8	−1477.47348	154.3	−1477.54677	3.76	
	TS(3–4)	26.2;*23.6*	182.2	24.3;*21.7*	153.1	24.8;*22.2*	3.22	
	4-S	6.5	183.8	6.0	152.7	6.6	3.07	432*i*
	4-T	2.5	184.0	2.8	156.1	1.7	3.11	
5[b]	**3**	−2451.84150		0		0	6.81	
	TS(3–4)	33.0;*31.4*		31.0;*28.4*		31.5	6.30	
	4-S	9.0		8.5		9.1	6.47	
	4-T	2.7		3.0		1.9	6.49	
6[b,c]	**3**	−11506.71587		0		0	13.57	
	TS(3–4)	31.6;*29.0*		29.6;*27.0*		30.1	13.10	
	4-S	8.4		7.9		8.5	13.60	
	4-T	2.3		2.6		1.5	13.61	

[a] Absolute energies, enthalpies, and free energies in Hartrees, corresponding differences ΔE, ΔH, ΔG in kcal mol^{-1}. For the triplets **4-T** the singlet triplet splitting is given. Zero point energies (ZPE) are in kcal mol^{-1}, entropies S in cal [mol K]$^{-1}$, dipole moments μ in debye, and imaginary frequencies ω in cm^{-1}. Values in normal print are B3LYP/3–21G optimized, values in italics are B3LYP/6–31G(d,p) optimized. [b] The thermochemical corrections of model 5 and model 6 structures were estimated on the basis of models 1–4. [c] Values for 6–31G(d,p) calculations are estimated.

Table 2. Energetics for the Bergman cyclization of the E-chair (E-C) conformation of (−)-calicheamicin γ_1^I (**1**).[a]

Model	Structure	E, ΔE	ZPE	H, ΔH	S	G, ΔG	μ	imag. ω
1	**3**	−1121.31705	143.9	−1121.07081	127.1	−1121.13121	3.25	
	TS(3–4)	22.2;*21.5*	142.9	21.8;*19.8*	119.7	22.7;*22.0*	2.46	437*i*
	4-S	1.6	144.2	1.1	119.5	3.4	2.84	
	4-T	2.7	144.2	2.9	122.8	1.9	2.86	
	TS(4–6)	22.2	141.9	20.0	120.4	19.8	2.82	483*i*
	6	−9.3	142.5	−10.0	126.1	−11.9	2.80	
2	**3**	−1196.10752	146.3	−1195.85677	126.7	−1195.91698	3.50	
	TS(3–4)	23.8;*22.2*	144.8	21.8;*20.2*	124.7	22.5;*20.9*	3.13	437*i*
	4-S	3.6	146.1	2.9	124.3	3.7	3.63	
	4-T	2.8	146.4	3.0	127.0	2.2	3.73	
	TS(4–6)	22.0	143.9	19.9	125.4	19.6	3.41	482*i*
	6	−9.0	144.5	−9.6	131.6	−11.8	3.76	
3	**3**	−1251.14818	156.7	−1250.87948	132.0	−1250.94221	3.67	
	TS(3–4)	22.5;*21.2*	155.3	20.6;*19.3*	129.8	21.2;*19.9*	3.00	429*i*
	4-S	1.2	156.9	0.6	128.6	1.6	3.67	
	4-T	2.2	157.1	2.5	130.5	1.9	3.79	
	TS(4–6)	22.8	154.3	20.6	132.1	19.2	2.85	480*i*
	6	−7.9	155.0	−8.6	137.2	−11.2	3.67	
4	**3**	−1477.78649	183.9	−1477.47028	155.0	−1477.54393	4.06	
	TS(3–4)	24.2;*22.7*	182.4	22.3;*20.8*	151.5	23.3;*21.8*	3.42	435*i*
	4-S	4.6;*−1.3*	183.8	3.9;*−1.9*	151.4	5.0;*−0.9*	4.07	
	4-T	2.8	183.5	3.1	154.8	2.0	4.15	
	TS(4–6)	22.0	181.5	19.9	152.8	19.5	3.96	484*i*
	6	−8.8	182.1	−9.5	159.1	−11.8	4.12	
5[b]	**3**	−2451.83353		0		0	7.11	
	TS(3–4S)	26.5;*22.2*		24.6;*20.3*		25.7;*24.4*	6.60	
	4-S	6.6		5.9		7.2	6.77	
	4-T	2.8		3.1		2.2	6.80	
	TS(4–6)	19.6		17.5		17.1	6.58	
	6	−8.0		−8.6		−10.8	6.72	
6[b,c]	**3**	−11506.71284		0		0	13.87	
	TS(3–4)	23.4;*21.4*		21.0;*19.1*		24.7;*23.2*	13.20	
	4-S	6.0		5.3		6.6	13.91	
	4-T	2.4		2.7		1.6	13.93	
	TS(4–6)	22.4		20.3		19.9	13.75	
	6	−11.9		−12.4		−13.8	13.90	

[a] Absolute energies, enthalpies, and free energies in Hartrees, corresponding differences ΔE, ΔH, ΔG in kcal mol^{-1}. For the triplets **4-T** the singlet triplet splitting is given. Relative values for **TS(4–6)** and **6** are with respect to **4-S**. Zero point energies (ZPE) are in kcal mol^{-1}, entropies S in cal [mol K]$^{-1}$, dipole moments μ in debye, and imaginary frequencies ω in cm^{-1}. Values in normal print correspond to B3LYP/3–21G//B3LYP/3–21G, values in italics to B3LYP/6–31G(d,p)//B3LYP/6–31G(d,p) energies. [b] The thermochemical corrections of model 5 structures were estimated on the basis of models 1–4. The 6–31G(d,p) values of models 5 were determined from single point calculations using the 3–21G optimized geometries. [c] Values for 6–31G(d,p) calculations are estimated.

the larger values resulting for the more-complete models. Using the 6–31G(d,p) basis leads to a decrease of 3 kcal mol^{-1} in the barrier. The most reliable value is 27.0 kcal mol^{-1} (model 6, that is, **3-Z-TB** without any simplifications). This barrier is too high to lead to any significant biological activity at body temperature. Accordingly, it is only of secondary interest that the Bergman reaction is endothermic by 7.9 kcal mol^{-1} and that the calculated S–T splitting is 2.6 kcal mol^{-1}.

The energetics of the Bergman cyclization of the (−)-enantiomer in the form of **3-Z-TB** is comparable to that of the parent enediyne **9**. The relatively high barrier is the result of a build-up of strain in **TS(3–4)**, which requires the formation of a cyclohexene half-chair conformation (enforced by the generation of the benzene ring) with the largest dihedral angle at the bond C12–C13 (see model 1, Scheme 2 and discussion in the Supporting Information).

The TB form cannot accommodate a large dihedral angle, which would imply $\phi_2 = 90°$ rather than 136°. (see Supporting Information). The requirements for an unstrained dihydrothiophene ring (primarily responsible for the TB form of **3-Z**) and the cyclohexene half-chair C2-C7-C8-C13-C12-C1 lead to a build-up of strain in the ring system, thus yielding a high activation enthalpy and an endothermic reaction enthalpy for the Bergman cyclization.

For **3-E-C**{180, 156} there are two reasons why a lower barrier should result: 1) The starting enediyne possesses 2 kcal mol^{-1} more strain (see Supporting Information), which is relieved in **TS(3–4)**, thus leading to a lower barrier. 2) The C form of the cyclohexanone ring can better accommodate a large dihedral angle at bond C12–C13 (60 vs. 30., see geometry data in the Supporting Information). These expectations are confirmed by the calculated activation enthalpies of the Bergman cyclization for **3-E-C** (Table 2), which are all around 20 kcal mol^{-1} at the B3LYP/6–31G(d,p) level

of theory. This would lead to a significant reaction rate at body temperature.

A recent study by Elmroth and co-workers[61] has shown that the ability of **1** to cause double-strand scission in DNA is not affected by the incubation temperature. This result is based on in vitro studies of calicheamicin cleavage of plasmid DNA at 0 and 37°C. For cellular DNA, the reduction to 0°C resulted in a loss of activity and this was proposed to be due to the impermeability of the cell by **1** at this temperature.[61] This observation implies an activation enthalpy lower than 19.6 kcal mol^{-1} at body temperature (requiring that 50% of the enediyne has reacted in less than 60 min for a ΔS^{a} of -3.5 cal [mol K]$^{-1}$; Table 2).

CCSD(T)/6–311G(d,p) calculations carried out for model 1 lead to an activation enthalpy of 17.1 kcal mol^{-1}, which is 2.7 kcal mol^{-1} lower than the best DFT value. Assuming the same lowering in the case of model 6, an activation enthalpy of 16.4 kcal mol^{-1} can be predicted, which is in line with the experimentally based estimate of Elmroth and co-workers.[61]

The Bergman reaction is almost thermoneutral (slightly endothermic at B3LYP/3–21G: 4 kcal mol^{-1}; slightly exothermic at B3LYP/6–31G(d,p): -2 kcal mol^{-1}, model 4; 5.3 kcal mol^{-1}, model 6; Table 2). The activation enthalpies for the two retro-Bergman reactions leading from biradical **4-S** back to **3** or forward to **6** are 16.3 and 20.3 kcal mol^{-1}, respectively (model 6, Table 2), with only little variation using one of the other models. The ring-opening reaction leading to enediyne **6** is exothermic by 12.4 kcal mol^{-1} (ΔH_{R}-(298) value of model 6), which means that a Bergman cyclization of **6** (to give **4-S**) has an activation enthalpy of 32.7 kcal mol^{-1}, that is, **6** resembles the parent enediyne in this respect[31] (see also Supporting Information).

We conclude that the singlet biradical **4-S** has a sufficiently long lifetime to abstract hydrogen atoms from DNA, which requires an activation enthalpy of less than 12 kcal mol^{-1}.[62] Its S–T splitting (ΔH(S–T) = 2.7 kcal mol^{-1}, model 6) is similar to that of *p*-benzyne[38] (see also Supporting Information).

The calculated energetics suggest that only **3-E-C** is biologically active, which should be formed in the Michael addition of **2** in a relatively small proportion. However, so far our investigation concerns exclusively the situation in the gas phase. The next section describes how the inclusion of solvent effects and consideration of the docking process change the situation substantially.

Investigation of the carbohydrate tail: The tail structure of **1** is composed of the five rings A, B, C, D, E and five connecting groups (ether, oxime, and thioester linkages). As the geometry of the rings is reasonably well constrained (essentially chair forms for the pyranose rings) this results in twelve rotatable bonds that can have a direct influence on the global shape of the tail and by this of the molecule. Thus, the long aryloligosaccharide tail of **1** has considerable flexibility compared to the constrained geometry of the bi/tricyclic head group and as such, the effect of the gas-phase geometry optimization on the tail structure requires special consideration.

For the determination of an aqueous-solution geometry, we started with the geometry that the tail has when embedded into the DNA as determined by MM/MD calculations and the NOE structure analysis of DNA–**1** complex.[31] By freezing the dihedral angles of the twelve linking bonds between the rings, the geometry of the tail was optimized at the B3LYP/3–21G level of theory. In a second step all degrees of freedom were relaxed, which led to a gradual back-rotation of the tail into the gas-phase geometry. Hence, we used the B3LYP/3–21G geometry with fixed dihedral angles as solution-phase geometry, in which the term solution phase is used in a wider sense considering that docking into the minor groove can also be seen as a specific solvation process accompanied by a change in nonspecific solvation.

In Figure 1, Connolly surfaces of the gas-phase and aqueous-solution geometries of **1** are shown, which reveal a large

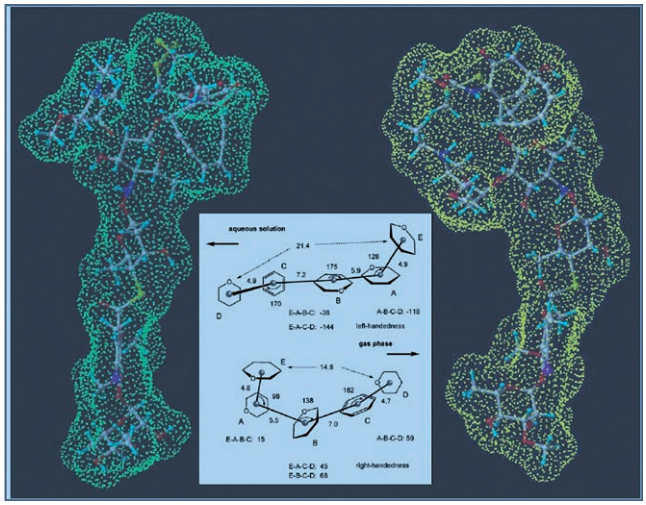

Figure 1. Representation of the carbohydrate tail of **1** according to its solution geometry (model 7, left; green Connolly surface) and its gas-phase geometry (model 6, right; yellow Connolly surface). In the middle the two geometries are simplified by representing each ring by its geometrical center and giving distances and angles between these centers for the solution and the gas-phase geometry. Looking from E to D the solution geometry (top) presents a left-handed, the gas-phase geometry (bottom) a right-handed screw. Distances in Å, angles in °.

difference similar to that between club and boomerang. The shape difference results from a deviating arrangement of rings A and E and a different tail curving. For the purpose of quantifying the latter, the tail section of **1** was reduced to a ring center representation by taking the geometrical center of each of the rings (E,A→D) to model the shape of the tail and to quantify the changes in the geometry upon solvation (Figure 1).

In the solution-phase geometry the tail is largely linear with some curling at the ends. Looking from ring E to ring D, the tail represents part of a left-handed helix (rotational angle -144°), which fits perfectly into the minor groove

with its right-handedness. The gas-phase geometry of the tail is strongly curled with a right-handedness (rotational angle of 68°), which does not fit into the minor groove (see also Figure 2). The solution structure is more extended as reflected by the distance E–D (21.4 vs. 14.8 Å, Figure 1), which also leads to a better fit with the minor groove.

Gas-phase and solution-phase geometry differ by 23.3 kcal mol^{-1}. The former is stabilized by intramolecular hydrogen bonding, which in the strongly curved form can develop better than in the extended form. For example, the position of ring A relative to rings B and the rest of the tail is strongly changed in the gas phase through the formation of a strong intramolecular hydrogen bond between a hydroxy substituent of ring A and the pyranose oxygen atom in ring B (H···O = 2.237 Å). This stabilizing hydrogen bond results in the decrease of the angle A-B-C from 175° in solution to 138° in the gas phase. In the Supporting Information details of the hydrogen-bond network in the two tail structures are given.

The dominance of the stretched out structure in aqueous solution is the result of three different effects: 1) Solvent calculations with the IPCM method and the dielectric constant of water ($\varepsilon = 78.4$[63]) for neutral **1** reveal that solvation stabilizes the extended geometry by at least 11 kcal mol^{-1} relative to the gas-phase geometry (this stabilization would be most likely larger if the ammonium cations would be compared). 2) Docking of the extended and the curled geometry to DNA leads to an energy difference of 14.9 kcal mol^{-1} (Table 3). 3) These trends will be enhanced by the effect that intramolecular hydrogen bonding will be partially replaced by intermolecular hydrogen bonding, which also leads to a stretching of the tail because hydrogen bonds between the rings responsible for the curling are broken. Although effects (1) and (2) cannot be simply added, it is likely that the stretched form of the tail becomes in the minor groove more stable than the gas-phase geometry, in line with the general understanding that extended structures with polar groups lead to stronger solvation in water.

These findings show clearly that there is no sense in using model 6 (the gas-phase geometry of **1**) in the docking investigation. A more realistic model of **1** (and **3**) is given by composite geometries containing the headgroup as determined by the DFT geometry optimizations (model 4) in connection with the tail geometry determined for the docking situation. The connection between headgroup and tail is forced to be that for the (−)- enantiomer (i.e., the tail is on the same side of the headgroup as the allyl trisulfide rest). Furthermore, attachment of the headgroup to the ring A of the aryl-oligosaccharide tail implies two possibilities; either attachment at the equatorial position of ring A (β anomer) or attachment at the axial position (α anomer). Experimentally, the β anomer has been shown to be the preferred structure (ratio β:α anomer is equal to 3:1[11b]), and, therefore, the attachment of the head group was made to the equatorial position of ring A. The composite structure obtained in this way is referred to as model 7 in the following.

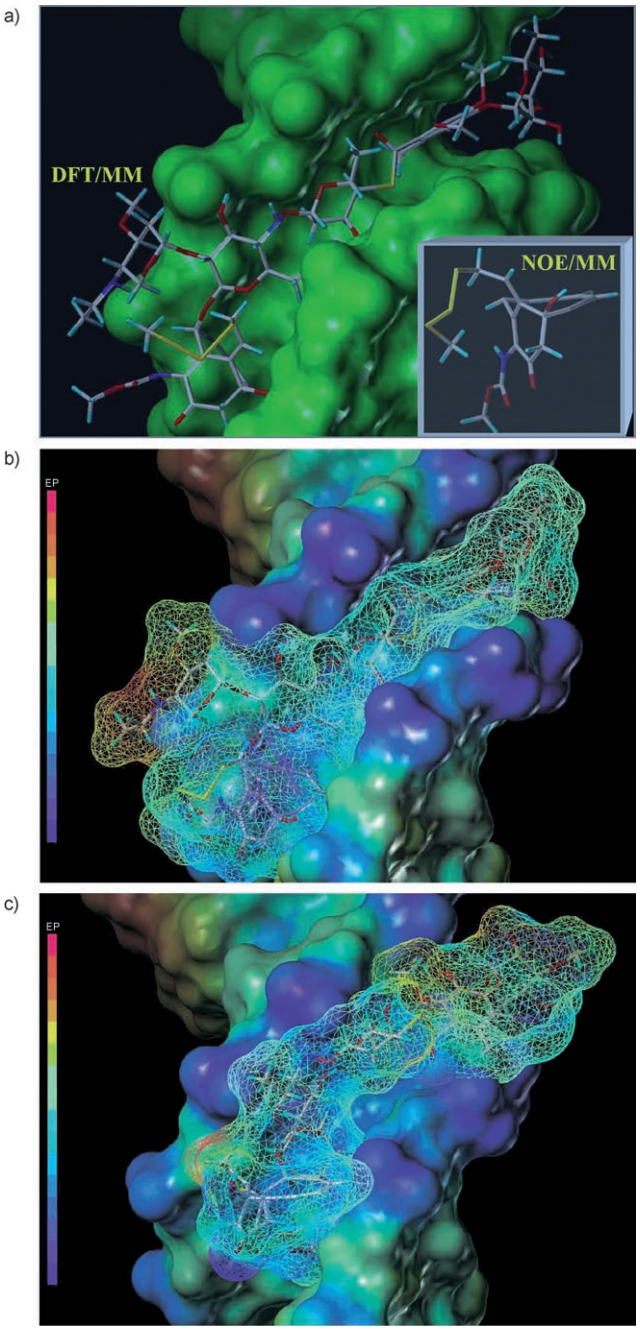

Figure 2. a) Positioning of calicheamicin γ_1^I (**1**) in the minor groove of the duplex 9mer-B-DNA sequence d(CACTCCTGG)·d(CCAGGAGTG). Molecule **1** is represented by a capped-stick model by using the geometry of model 7 (composite geometry), whereas DNA is depicted by its Connolly surface. The insert gives the headgroup of the NOE/MM structure[31] for reasons of comparison. b) The NOE/MM structure of **1** docked into the minor groove of DNA. The electrostatic potential (EP) is projected on the Connolly surfaces of ligand and receptor where in the former case the net representations of the surface provides an insight into the structure of the ligand. On the left, a color scale of the EP is given. c) The gas-phase structure of **1** docked into the minor groove of DNA. Again, the EP projected on the Connolly surfaces of ligand and receptor are given.

Docking into the minor groove of DNA: The NOE/MM structure of **1** (PDB ID: 2PIK-5)[31] was docked into the

Table 3. Docking energies ΔE_b, inhibition constants K_i, hydrogen-abstraction sites, and the abstraction distances of the *E*-chair (E-C) and *Z*-twistboat (Z-TB) conformers resulting from a triggering of (−)-calicheamicin γ_1^I (**1**).[a]

Molecule	Conformation	Source	ΔE_b	K_i	Abs. site C3	C3···H	Abs. site C6	C6···H
1		NOE/MM[b]	−13.35	1.63×10^{-10}	C5(H5′)	3.159	G23(H5′)	2.764
1		model 7	−12.51	6.72×10^{-10}	C5(H5′)	2.346	G23(H5′)	3.694
1		model 6	2.35					
3	**Z-TB**	model 7	−14.37	2.93×10^{-11}	C5(H5′)	3.447	G23(H5′)	2.557
TS(3–4)	**Z-TB**	model 7	−13.78	7.99×10^{-11}	C5(H5′)	3.549	G23(H5′)	2.506
4-S	**Z-TB**	model 7	−13.56	1.15×10^{-10}	C5(H5′)	3.156	G23(H5′)	3.021
3	**E-C**	model 7	−14.38	2.86×10^{-11}	C5(H5′)	3.068	T22(H4′)	2.597
TS(3–4)	E-C	model 7	−13.68	9.41×10^{-11}	C5(H5′)	2.263	T22(H4′)	3.854
4-S	**E-C**	model 7	−13.64	9.99×10^{-11}	C5(H5′)	2.245	T22(H4′)	3.898

[a] All calculations refer to the *S*,*R* configuration and the β anomer. Energy differences in kcal mol^{-1}, inhibition constants in mol, distances in Å. C···H denotes the distance between the proradical C atom and the closest hydrogen atom. Abs. site is the abstraction site, indicating the nucleotide and the hydrogen aligned for abstraction. [b] Ref. [31].

minor groove of the duplex 9mer-B-DNA sequence d(CACTCCTGG)·d(CCAGGAGTG) to serve as a reference for the binding energies calculated by AutoDock. The orientation of the docked position of the reference molecule is, to all intents and purposes, identical to that of the refined NOE structure.[31] This fact is evident in the alignment of the proradical carbon atoms of the warhead with the hydrogen abstraction sites (C5(H5′) and G23(H5′)) aligned in the refined complex.[31] The binding energy calculated ($\Delta E_b = -13.35$ kcal mol^{-1}; Table 3) results in an inhibition constant ($K_i = 1.63\times10^{-10}$) that is actually smaller than can be expected in view of the nanomolar activity found for the drug.[4]

When using our DFT optimized composite geometry (model 7), a K_i value of 6.7×10^{-10} mol is calculated (($\Delta E_b = -12.5$ kcal mol^{-1}, Table 3), which is a factor of 5×10^{-3} smaller (ΔE_b is 2.8 kcal mol^{-1} larger, that is, more negative) than the experimental value of 1.35×10^{-7} ($\Delta G_{binding} = -9.7$ kcal mol^{-1}) given by Nicolau and co-workers.[27] Such a difference is expected because of the simplifications we had to make in this work: 1) We do not consider entropy changes included into the experimentally obtained free docking energies ΔG (see Computational Methods and Strategies Section). There will be a decrease in entropy upon docking, which in itself is partially reduced by the fact that intercalated water molecules are forced out of the minor groove.[31,55] Moreover, the ligand will loose part of its solvent shell upon entering the minor groove, which again increases entropy. Considering all effects, entropy should reduce the absolute value of the docking energy, thus leading to a better agreement between theory and experiment. Clearly, future studies have to include solvent effects explicitly and must consider a reoptimization of the complex not possible in this work.

However, in the present work we are concerned primarily with the relative changes in the binding energy during the Bergman cyclization, for which the above-mentioned simplifications are expected to play only a minor role.

Figure 2a shows the docking of **1** (model 7) into the minor groove of DNA, where the former is represented by a capped-stick model and the latter by a Connolly surface. Also shown in an insert is part of the headgroup as described in the NOE/MM structure.[31] Comparison reveals that the carbamate group has a different orientation in the two structures. DFT orients the carbamate group perpendicular to the cyclohexenone ring (Figure 2a) to establish a hydrogen bond (electrostatic attraction) between the methyl group of the allyl sulfide and the keto-oxygen of the carbamate group. In this way, also an unfavorable Y conjugation of the carbamate group with the dieneone system is avoided. The NOE/MM structure, however, keeps the carbamate group planar with regard to the ring, provoking in this way an unfavorable keto–keto interaction (insert of Figure 2a), but reducing repulsive interactions between the NH of the carbamate group and proximal CH bonds of DNA. Also, the trisulfide can arrange better in the minor groove.

For the NOE/MM structure[31] the docking situation is slightly better, although the orientation of the carbamate and trisulfide substituents in the headgroup implies a much larger intramolecular destabilization of **1**. Here the importance of a DFT rather than a MM description becomes apparent, which is even more obvious in discussing the special role of the carbamate group.

The overall docking orientation of the NOE/MM structure and the DFT structure (model 7) of **1** are similar, as documented by Figure 2b, which shows the capped-stick representation of the NOE/MM structure enveloped into the electrostatic potential (EP) mapped on the Connolly surface of the molecule, indicated by a suitable color code (negatively charged parts blue, neutral parts green, positively charged parts red, see scale on the left of Figure 2b), and embedded into the minor groove of the DNA, where again the Connolly surface carries the color-coded EP information.

Contrary to expectations found in the literature,[4] there is no strong electrostatic attraction between **1** and DNA apart from the alignment of the $R-NH_2^+$ group of ring E with one of the negatively charged phosphate groups of DNA (see red-yellow colored part on the left side of the headgroup of **1** in Figure 2b). This interaction results in a salt bridge or better in the formation of a strong ionic hydrogen bond $N-H^+\cdots O^-$ linkage. Considering the distance between these groups (O···H = 1.759 Å) the resulting ionic hydrogen

bond would lead to an attraction energy in the gas phase with an upper limit of 188 kcal mol^{-1} that is reduced to about 40 kcal mol^{-1} due to the fact that positive and negative charge are spread over several atoms, and to about 10 kcal mol^{-1} considering the damping factor of the surrounding solvent (a dielectric constant of 4 is assumed).

For the purpose of getting a more accurate guess on the effect of the salt bridge two different calculations were carried out. 1) The interaction energy between NH_4^+ and $H_2PO_4^-$ arranged at a O···H distance of 1.759 Å was calculated to be 10.4 kcal mol^{-1} in a polarizable continuum with $\varepsilon = 78.4$ at B3LYP/6–31G(d,p). 2) The docking of **1** was repeated changing, however, the positive ethylammonium group into a neutral ethyl amino group. The docking energy obtained in this way is 1.2 kcal mol^{-1} less. We can consider the two values obtained in this way as upper and lower boundaries of the true interaction energy between ethylammonium and phosphate ion: the first value is exaggerated by basis set superposition error and the absence of specific solvation effects, whereas the second value is underestimated by reorientation of neutral **1** in the minor groove so to compensate for the loss of the salt bridge.

Docking of **1** using its gas-phase geometry (model 6, see Figure 2c) leads to a noncomplimentary fit between the ligand and the DNA, as reflected by the positive binding energy of the interaction ($\Delta E_b = 2.35$ kcal mol^{-1}; Table 3). As discussed in the previous section the handedness of model 6 does not comply with that of DNA. Accordingly, there is an arching of the gas-phase tail out of the minor groove and the entire head unit extends beyond the global shape of the DNA (Figure 2c). This is another example of the fact that gas-phase conformations of flexible molecules are of little relevance for determining which conformation is adopted in aqueous solution.

The composite structures (model 7) of the Bergman cyclization reaction for both the TB and the C conformations of the cyclohexanone ring were docked into the minor groove of the DNA, with identical binding energies for the different conformations (e.g., **3-Z-TB** and **3-E-C**: $\Delta E_b = -14.4$ kcal mol^{-1}; Table 3). Thus, we find that energetically there is no preference in the binding mode between the **Z-TB** or **E-C** conformers, which means that the destabilization of the latter form by 1.9 kcal mol^{-1} (see Supporting Information) is not compensated by the docking process. This is also true with regard to **TS(3–4)** and biradical **4-S**: Throughout the Bergman cyclization, the difference in the binding energies of the **Z-TB** and **E-C** forms are so small (maximally 0.1 kcal mol^{-1}) that they cannot change the conclusions based on strain effects. This would still mean that the biological activity is exclusively constrained to the **3-E-C** form, only a small proportion of which is formed.

There is, however, a clear difference between **4-S-Z-TB** and **4-S-E-C** as far as the alignment of the radical carbon atoms with the hydrogen abstraction sites is concerned. Both conformers abstract first H5′ of the ribose attached to C5 (cytosine 5). However, the phenyl radical formed out of **4-S-Z-TB** should abstract next H5′ of G23 (guanine 23), whereas the phenyl radical formed out of **4-S-E-C** should abstract H5′ of T22 (thymine 22), in which only the latter result is in line with experimental observations.[18–21]

The results summarized in Table 3 make it necessary to reconsider the triggering mechanism for the purpose of solving the contradiction between experimental observations and theoretical predictions.

Reconsideration of the stereochemistry of the Michael addition: In Figure 3a, that part of the headgroup of **1** is enlarged that shows allyltrisulfide, carbamate group, cyclohexenone ring, and the enediyne unit embedded in the minor groove. The carbamatetrisulfide interaction distance (2.153 Å at B3LYP/3–21G) is indicated by a dashed yellow line. The direction of the nucleophilic attack of a glutha-

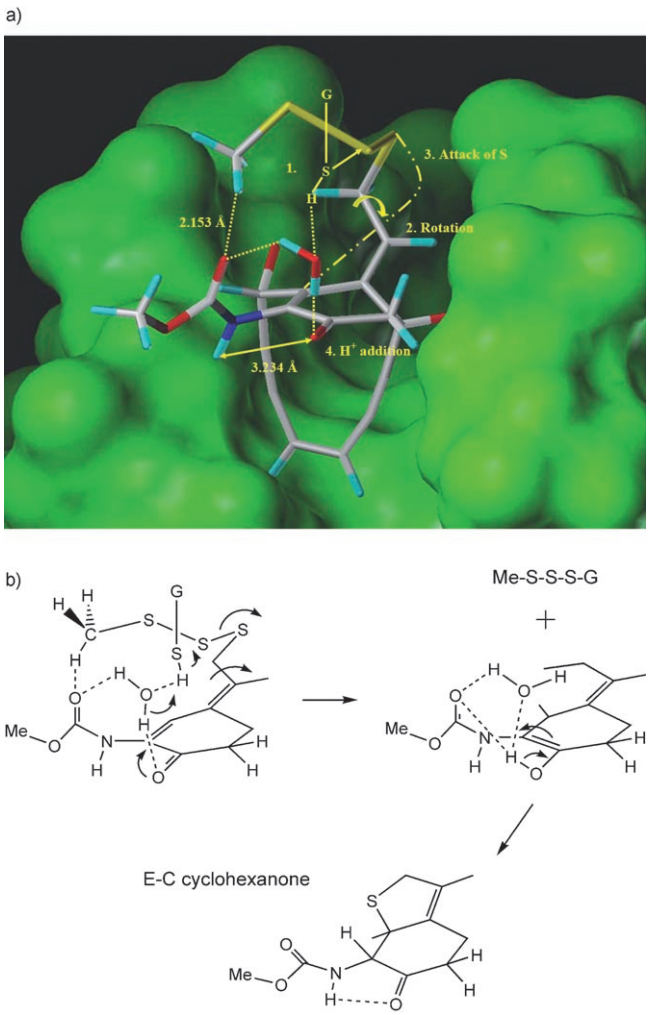

Figure 3. a) The headgroup of **1** (model 7) is shown in the minor groove of DNA to explain the stereochemistry of the Michael addition. the various steps (1. nucleophilic attack by gluthathione at the S–S bond; 2. rotation at the C–C bond; 3. attack of S at the cyclohexenone double bond; 4. proton addition at the enolate oxygen) are schematically indicated. b) Enolate/enol formation and enol–keto tautomerization as catalyzed by a water molecule. The back of the cyclohexenone/cyclohexanone ring (connections to enediyne unit and to sugar tail) is not completely shown to avoid confusion.

thione molecule at the SS bond (step 1) is also shown. Glutathione has a pK_a value of 8.75 for the SH group in aqueous solution,[63] which means that at pH 7 almost 97% of glutathione is in the acidic SH form. Upon SS bond cleavage (yielding MeSSSG and $^-$S–R), the sulfide anion will capture a proton from somewhere, leave in the direction to the tail and, because it is bonded to a C atom, its linear momentum will be converted to an angular momentum, that is, there will be a rotation at the CC bond, as indicated in Figure 3 (step 2), which helps the new thiol to attack the double bond from above (step 3).

The enolate anion that is formed can be protonated at the oxygen atom from above or below. However, there should be a preference for a topside protonation because (a) water molecule(s) will sit there, hydrogen bonded to both the enolate anion and the keto oxygen of the carbamate group (see Figure 3a and b). This water molecule will be perfectly located to accept a proton from gluthathione and to donate a proton to the enolate oxygen. The enol formed is hydrogen bonded to the water molecule that then functions as a catalyst for the enol–keto tautomerization, which is completed with a rotation of the carbamate group into the plane of the keto group of cyclohexanone so that a NH···O=C intramolecular hydrogen bond can be formed (see Figure 3b).

Assistance of a water molecule (or two) sitting on the topside of the cyclohexanone ring rather than on the bottomside (the proximity of NH and C=O group makes the formation of a water complex more difficult and a proton has to be taken from somewhere else rather than the gluthathione molecule) will lead to a protonation at C11 from the topside. Therefore, the enol–keto tautomerization will preferentially yield the **3-E-C** rather than the **3-Z-TB** conformer contrary to what one would expect in view of the thermodynamic stabilities of the two conformers. This, of course, is of utmost importance for the biological activity of **1** (see below).

Chemical Relevance of Results

Due to the DFT description of **1** we find an orientation of the carbamate group that differs essentially from that used in previous descriptions.[31] This has serious consequences for both the triggering mechanism and the Bergman cyclization:

1) In the minor groove, the Michael addition leads, because of the catalytic effect of water located at the topside of the cyclohexenone ring, to a preferential formation of the E-C cyclohexanone ring of the triggered form **3** (Supporting Information).
2) Only **3-E-C** has a sufficiently low barrier for Bergman cyclization (16.4 kcal mol^{-1}) to become active at body temperature. The conformer **3-Z-TB** will not react. The lowering of the barrier is because the chair form of the cyclohexanone ring can better accommodate an annelated halfchair form in the neighboring ring (required by the benzene formed), whereas it itself is slightly destabilized by additional strain (2 kcal mol^{-1}), as discussed above.
3) The biradical **4-S-E-C** is kinetically stable because the barriers for retro-Bergman reactions (16 and 20 kcal mol^{-1}, Table 2) are considerably larger than the barrier for hydrogen abstraction from DNA (estimated to be $\leq$12 kcal mol^{-1}[62]).
4) The docking investigation leads to an inhibition constant of 6.7×10^{-10} mol and a complexation energy of -12.5 kcal mol^{-1}. Comparison with experiment suggests that there is an increase in entropy by 9 cal[mol K]$^{-1}$, which would lead to the experimental values of $K_i = 1.35\times10^{-7}$ mol and $\Delta G_b = -9.7$ kcal mol^{-1}.[27]

We note that the NOE/MM structure of **1**[31] contains a questionable positioning of the carbamate group, which lowers intermolecular repulsion but misses the important possibility of hydrogen bonding between trisulfide and carbamate group.

Triggering of **1** leads to improved docking, as is reflected by a complexation energy of -14.4 kcal mol^{-1} and an inhibition constant of 3×10^{-11} mol (Table 3). This suggests that once docked and triggered there is little chance that calicheamicin leaves the minor groove. Furthermore, the orientation of the head group of **3-E-C** in the minor groove is slightly rotated from that of **1** so that the proradical carbon atoms are aligned with the hydrogen abstraction sites that have experimentally been shown to be the preferred abstraction sites, C5(H5′) and T22(H4′) (see Table 3), for this particular DNA sequence.[4,31]

Once triggered, the Bergman cyclization reaction will occur spontaneously, which requires that the ligand remains docked in the DNA throughout the cyclization process. Therefore, all intermediate structures in the hydrogen-abstraction process were considered by using model 7. There is a 0.8 kcal mol^{-1} decrease of the docking energy to -13.6 kcal mol^{-1} in the Bergman cyclization (Table 3). The overall orientation of **3** in the minor groove is not affected during the cyclization reaction. However, during the Bergman cyclization there is some further rotation of the headgroup within the minor groove, which results in the preference of one abstraction site over the other.

The formation of **4-S-E** accentuates the preference for the initial abstraction by the C3 atom of the warhead. The preference for the abstraction of the C5(H5′) atom over the T22(H4′) atom is larger, as reflected by the alignment of the radical C atoms with the corresponding CH bonds (C3···H = 2.245, C6···H = 3.898 Å; Table 3 and Figure 4). The relative C···H distances indicate that the abstraction process will occur in two distinct steps. The C5(H5′) atom will be abstracted by the C3 radical and this will then lead to a realignment of the warhead to abstract the second hydrogen atom from T22(H4′). This is in contrast to previous proposals, which were based only on the alignment of the untriggered structure, and suggested that the abstraction of both hydrogen atoms would occur concomitantly.[4,31] Thus, the

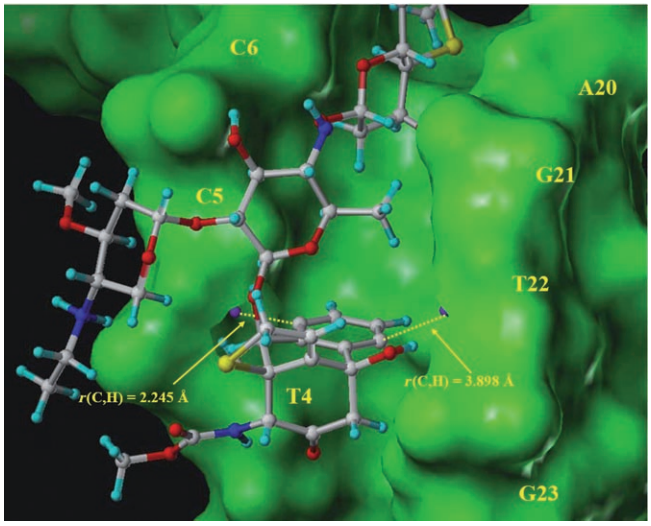

Figure 4. Docking of the singlet biradical **4-S-E** (capped stick representation) into the minor groove of DNA represented by a Connolly surface. The sequence of DNA is indicated. The proximal hydrogen atoms to be abstracted are made visible. In the first step the C5H5′ atom will be abstracted by the C3 radical (distance r(C,H) = 2.245 Å), in the second step the hydrogen atom T22H4′ (r(C,H) = 3.898 Å) by C6.

consideration of only the untriggered structure **1** in the minor groove leads to an incorrect description of the abstraction mechanism, to correctly describe this process the species involved in the hydrogen abstraction (i.e., biradical **4-S-E-C**) must be considered.

Does calicheamicin react preferentially in the minor groove? There are two answers that can be mentioned here: 1) If **1** is fixed in the minor groove and in addition the trisulfide group by intramolecular hydrogen bonding with the carbamate group, the probability of reactive collisions is increased. Outside the minor groove the movements of **1** and thiol coupled with rotations of the allyltrisulfide group reduce the probability of reactive collisions, which require a nucleophilic attack in the direction of the S–S bond adjoining the allyl function. This should be more difficult considering the flip-flop rotations of a trisulfide[64] (suppressed by hydrogen bonding in the minor groove). 2) Outside the minor groove the Michael addition should lead preferentially to the thermodynamically more stable **3-Z-TB** conformer rather than the **3-E-C** conformer, because outside the minor groove there is no longer any reason that protonation should preferably take place at the topside of the cyclohexenone ring (side of the new C–S bond), as discussed above. The **3-Z-TB** conformer has, however, a barrier to Bergman cyclization, which under normal conditions cannot be surmounted at body temperature, whereas the **3-E-C** conformer has a 10 kcal mol^{-1} lower barrier and, therefore, reacts with a sufficiently large rate at body temperature.

One could, however, argue that in the triggering process so much energy is set free that it does not matter whether the activation enthalpy is 27 or 19 kcal mol^{-1}. Also in this context it must be asked why the energy set free is not sufficient to undock the molecule. If there is an equilibrium between docking and undocking, any excess energy in an amount required for the Bergman reaction should be also sufficient for the much smaller energy required for undocking (13.4 kcal mol^{-1}; experimentally 9.7 kcal mol^{-1}[27]).

In this connection we have to consider the possibility of energy dissipation. In the triggering reaction a total of 48 kcal mol^{-1} are set free, however, this is done in several steps considering that first a sulfide anion (more likely a thiol) is formed, then a new C–S bond, followed by protonation at an enolate oxygen, reprotonation, and protonation of a carbanion. The excess energy will be first dissipated by distribution among vibrational modes yielding a (locally) hot molecule.

Outside the minor groove the molecule is cooled down by collisions with solvent molecules, which should be a rapid process. However, inside the minor groove cooling is slowed down as the DNA template cannot function as effectively as the water molecules do. Therefore, the chance increases that also those framework vibrations of **1** that initiate the Bergman cyclization are activated. There is accordingly competition between a vibration-controlled Bergman cyclization and a diffusion-controlled undocking process (both fuelled by the excess energy) in which clearly the Bergman cyclization should be faster than undocking.

We conclude that 1) the preferential formation of the **3-E-C** conformer and 2) the lack of rapid dissipation of the triggering excess energy are responsible for the fact that the Bergman product, the singlet biradical **4-S** is formed to an appreciable amount only inside the minor groove. If it is formed to a small percentage outside the minor groove (where **3-Z-TB** should be preferentially formed), then it will abstract almost arbitrarily hydrogen atoms from molecules encountered in its collision course and these molecules (solvent, amino acid, protein molecules, etc.) are not necessarily vital for cell survival.

This work has shed further light on the biological activity of the natural enediyne **1**. Compound **1** is actually toxic and, therefore, considerable care has to be taken to use it as an antitumor drug, although several attempts in this direction have been undertaken.[4] An absolute prerequisite for the design of any antitumor drug based on the biological activity of **1** is the understanding of the reactivity of **1** in the cell. Despite the fact that numerous experimental studies have been carried out to describe the chemical and biological behavior of this compound,[1–4] this investigation proves that quantum chemistry can provide important assistance in these investigations, provided the emphasis is more on reliable quantum chemical methods, such as DFT, rather than MM descriptions. Clearly, DFT is superior to MM when hydrogen bonding,[65] π conjugation, biradical character, charge delocalization, or strain effects have to be described. We consider our investigation to be guiding in two ways: 1) DFT must play a stronger role in biochemical QM/MM investigations than it has done so far. 2) The choice of the model must be taken more carefully as done in many other similarly motivated studies. Only by using a series of models

(models 1 to 7), was the decisive role of the carbamate group for the triggering mechanism discovered in this investigation.

Because we consider that some basic questions in connection with the calicheamicin problem are now solved, we have started work to design a new nontoxic antitumor drug with increased biological activity based on the calicheamicin principle. In view of the recent approval of **1** for the clinical treatment of leukemia,[66] our investigation is timely and will hopefully accelerate the use of **1** as an antitumor drug.

Acknowledgement

E.K. and D.C. thank the University of the Pacific for generous support of this work.

[1] a) K. C. Nicolaou, W.-M. Dai, *Angew. Chem.* **1991**, *103*, 1453; *Angew. Chem. Int. Ed. Engl.* **1991**, *30*, 1387; b) K. C. Nicolaou, A. L. Smith, E. W. Yue, *Proc. Natl. Acad. Sci. USA* **1991**, *88*, 7464; c) K. C. Nicolaou, A. L. Smith, E. W. Yue, *Proc. Natl. Acad. Sci. USA* **1993**, *90*, 5881.
[2] J. S. Thorson, E. L. Sievers, L. Ahlert, E. Shepard, R. E. Whitwam, K. C. Onwueme, M. Ruppen, *Curr. Pharm. Des.* **2000**, *6*, 1841.
[3] G. Saito, J. A. Swanson, K.-D. Lee, *Adv. Drug Delivery Rev.* **2003**, *55*, 199.
[4] D. B. Borders, T. W. Doyle, *Enediyne Antibiotics as Antitumour Agents*, Marcel Decker, New York, **1995**.
[5] G. A. Lee, M. D. Ellestad, D. B. Borders, *Acc. Chem. Res.* **1991**, *24*, 235.
[6] a) M. D. Lee, T. S. Dunne, M. M. Siegel, C. C. Chang, G. O. Morton, D. B. Borders, *J. Am. Chem. Soc.* **1987**, *109*, 3464; b) M. D. Lee, T. S. Dunne, C. C. Chang, G. A. Ellestad, M. M. Siegel, G. O. Morton, W. J. McGahren, D. B. Borders, *J. Am. Chem. Soc.* **1987**, *109*, 3466.
[7] D. Kahn, D. Yang, M. D. Lee, *Tetrahedron Lett.* **1990**, *31*, 21.
[8] M. D. Lee, T. S. Dunne, C. C. Chang, M. M. Siegel, G. O. Morton, G. A. Ellestad, W. J. McGahren, D. B. Borders, *J. Am. Chem. Soc.* **1992**, *114*, 985.
[9] a) A. L. Smith, C.-K. Hwang, E. Pitsinos, G. Scarlato, K. C. Nicolaou, *J. Am. Chem. Soc.* **1992**, *114*, 3134. The first, although not enantioselective, synthesis was carried out by b) M. Paz Cabel, R. S. Coleman, S. J. Danishefsky, *J. Am. Chem. Soc.* **1990**, *112*, 3253.
[10] K. C. Nicolaou, C. W. Hummel, E. N. Pitsinos, M. Nakada, A. L. Smith, K. Shibayama, H. Saimoto, *J. Am. Chem. Soc.* **1992**, *114*, 10082.
[11] a) J. Aiyer, S. A. Hitchcock, D. Denhart, K. K. C. Liu, S. J. Danishefsky, D. M. Crothers, *Angew. Chem.* **1994**, *106*, 925; *Angew. Chem. Int. Ed. Engl.* **1994**, *33*, 855; b) S. A. Hitchcock, S. A. Boyer, M. Y. Chu-Moyer, S. Olson, S. F. Danishefsky, *Angew. Chem.* **1994**, *106*, 928; *Angew. Chem. Int. Ed. Engl.* **1994**, *33*, 858.
[12] D. L. J. Clive, Y. Bo, N. Selvakumar, R. McDonald, B. D. Santarsiero, *Tetrahedron* **1999**, *55*, 3277.
[13] R. G. Bergman, *Acc. Chem. Res.* **1973**, *6*, 25.
[14] a) T. P. Lockhart, P. B. Comita, R. G. Bergman, *J. Am. Chem. Soc.* **1981**, *103*, 4082; b) T. P. Lockhart, R. G. Bergman, *J. Am. Chem. Soc.* **1981**, *103*, 4090.
[15] H. Kishikawa, Y. P. Jiang, J. Goodisman, J. C. Dabrowiak, *J. Am. Chem. Soc.* **1991**, *113*, 5434.
[16] J. Drak, W. A. N. Wasa, S. Danishefsky, D. M. Crothers, *Proc. Natl. Acad. Sci. USA* **1991**, *88*, 7464.
[17] a) N. Zein, A. M. Sinha, W. J. McGahren, G. A. Ellestad, *Science* **1988**, *240*, 1198; b) N. Zein, M. Poncin, G. A. Nilakantin, *Science* **1989**, *244*, 697.
[18] J. J. De Voss, C. A. Townsend, W. D. Ding, G. O. Morton, G. A. Ellestad, N. Zein, A. B. Tabor, S. L. Schreiber, *J. Am. Chem. Soc.* **1990**, *112*, 9669.
[19] a) S. C. Mah, C. A. Townsend, T. D. Tullius, *Biochemistry* **1994**, *33*, 614; b) S. C. Mah, M. A. Price, C. A. Townsend, T. D. Tullius, *Tetrahedron* **1994**, *50*, 1361.
[20] N. Zein, W. J. McGahren, G. O. Morton, J. Ashcroft, G. A. Ellestad, *J. Am. Chem. Soc.* **1989**, *111*, 6888.
[21] S. Walker, R. Landovitz, W. D. Ding, G. A. Ellestad, D. Kahne, *Proc. Natl. Acad. Sci. USA* **1992**, *89*, 4608.
[22] J. J. Hangeland, J. J De Voss, J. A. Heath, C. A. Townsend, W. D. Ding, J. S. Ashcroft, G. A. Ellestad, *J. Am. Chem. Soc.* **1992**, *114*, 9200.
[23] P. C. Dedon, A. A. Salzberg, J. Xu, *Biochemistry* **1993**, *32*, 3617.
[24] C. Liu, B. M. Smith, K. Ajito, H. Komatsu, L. Gomez-Paloma, T. Li, E. Theodorakis, K. C. Nicolaou, P. K. Vogt, *Proc. Natl. Acad. Sci. USA* **1996**, *93*, 940.
[25] A. Kalben, S. Pal, A. H. Andreotti, S. Walker, D. Gange, K. Biswas, D. Kahne, *J. Am. Chem. Soc.* **2000**, *122*, 8403.
[26] K. Biswas, S. Pal, J. D. Carbeck, D. Kahne, *J. Am. Chem. Soc.* **2000**, *122*, 8413.
[27] T. Li, Z. Zeng, V. A. Estevez, K. U. Baldenius, K. C. Nicolaou, G. F. Joyce, *J. Am. Chem. Soc.* **1994**, *116*, 3709.
[28] a) S. Walker, J. Murnick, D. Kahne, *J. Am. Chem. Soc.* **1993**, *115*, 7954; b) S. Walker, D. Yang, D. Kahne, *J. Am. Chem. Soc.* **1991**, *113*, 4716.
[29] N. Ikemoto, A. Kumar, T. Ling, G. A. Ellestad, S. J. Danishefsky, D. J. Patel, *Proc. Natl. Acad. Sci. USA* **1995**, *92*, 10506.
[30] L. G. Paloma, J. A. Smith, W. J. Chazin, K. C. Nicolaou, *J. Am. Chem. Soc.* **1994**, *116*, 3697.
[31] R. A. Kumar, N. Ikemoto, D. J. Patel, *J. Mol. Biol.* **1997**, *265*, 187.
[32] R. Lindh, U. Ryde, M. Schütz, *Theor. Chem. Acc.* **1997**, *97*, 203.
[33] a) R. Rothchild, A.-M. Sapse, A. Balkova, J. W. Lown, *J. Biomol. Struct. Dyn.* **2000**, *18*, 413; b) A.-M. Sapse, R. Rothchild, W. J. Lown, *J. Biomol. Struct. Dyn.* **2000**, *18*, 423.
[34] S. Felgdus, G. C. Shields, *Chem. Phys. Lett.* **2001**, *347*, 505.
[35] E. Kraka, D. Cremer, *J. Am. Chem. Soc.* **1994**, *116*, 4929.
[36] E. Kraka, D. Cremer, *Chem. Phys. Lett.* **1993**, *216*, 333.
[37] R. Marquardt, A. Balster, W. Sander, E. Kraka, D. Cremer, J. G. Radziszewski, *Angew. Chem.* **1998**, *110*, 1001; *Angew. Chem. Int. Ed.* **1998**, *37*, 955.
[38] J. Gräfenstein, A. Hjerpe, E. Kraka, D. Cremer, *J. Phys. Chem. A* **2000**, *104*, 1748.
[39] E. Kraka, D. Cremer, *J. Mol. Struct.: THEOCHEM* **2000**, *506*, 191.
[40] E. Kraka, D. Cremer, *J. Comput. Chem.* **2000**, *22*, 216.
[41] B. Ahlström, E. Kraka, D. Cremer, *Chem. Phys. Lett.* **2002**, *361*, 129.
[42] T. Tuttle, E. Kraka, D. Cremer, *J. Am. Chem. Soc.* **2005**, *127*, 9469.
[43] E. Kraka, D. Cremer, *J. Am. Chem. Soc.* **2000**, *122*, 8245.
[44] P. C. Hariharan, J. A. Pople, *Theor. Chim. Acta.* **1973**, *28*, 213.
[45] J. S. Binkley, J. A. Pople, W. J. Hehre, *J. Am. Chem. Soc.* **1980**, *102*, 939.
[46] A. D. Becke, *J. Chem. Phys.* **1993**, *98*, 5648.
[47] A. D. Becke, *Phys. Rev. A* **1988**, *38*, 3098.
[48] C. Lee, W. Yang, R. G. Parr, *Phys. Rev. B* **1988**, *37*, 785.
[49] a) R. Seeger, J. A. Pople, *J. Chem. Phys.* **1977**, *66*, 3045; b) R. Bauernschmitt, R. Ahlrichs, *J. Chem. Phys.* **1996**, *104*, 9047.
[50] J. B. Foresman, A. Keith, K. B. Wiberg, J. Snoonian, M. J. Frisch, *J. Phys. Chem.* **1996**, *100*, 16098.
[51] COLOGNE2006, E. Kraka, J. Gräfenstein, M. Filatov, Y. He, J. Gauss, A. Wu, V. Polo, L. Olsson, Z. Konkoli, Z. He, D. Cremer, Göteborg University, Göteborg, **2003**.
[52] M. J. Frisch, G. W. Trucks, H. B. Schlegel, G. E. Scuseria, M. A. Robb, J. R. Cheeseman, V. G. Zakrzewski, J. A. Montgomery, Jr., R. E. Stratmann, J. C. Burant, S. Dapprich, J. M. Millam, A. D. Daniels, K. N. Kudin, M. C. Strain, O. Farkas, J. Tomasi, V. Barone, M. Cossi, R. Cammi, B. Mennucci, C. Pomelli, C. Adamo, S. Clifford, J. Ochterski, G. A. Petersson, P. Y. Ayala, Q. Cui, K. Morokuma, D. K. Malick, A. D. Rabuck, K. Raghavachari, J. B. Foresman, J. Cioslowski, J. V. Ortiz, A. G. Baboul, B. B. Stefanov, G. Liu, A. Liashenko,

P. Piskorz, I. Komaromi, R. Gomperts, R. L. Martin, D. J. Fox, T. Keith, M. A. Al-Laham, C. Y. Peng, A. Nanayakkara, C. Gonzalez, M. Challacombe, P. M. W. Gill, B. G. Johnson, W. Chen, M. W. Wong, J. L. Andres, M. Head-Gordon, E. S. Replogle, J. A. Pople, Gaussian, Inc., Gaussian98, Revision A3, Pittsburgh PA, **1998**.

[53] D. Cremer, J. A. Pople, *J. Am. Chem. Soc.* **1975**, *97*, 1354.

[54] D. Cremer, *J. Phys. Chem.* **1990**, *94*, 5502.

[55] G. M. Morris, D. S. Goodsel, R. S. Halliday, R. Huey, W. E. Hart, R. K. Belew, A. J. Olson, *J. Comput. Chem.* **1998**, *19*, 1639.

[56] a) M. L. Connolly, *Science* **1983**, *221*, 709; b) M. L. Connolly, *J. Appl. Crystallogr.* **1983**, *16*, 548.

[57] Y.-R. Luo, *Handbook of Bond Dissociation Energies in Organic Compounds*, CRC Press, New York, **2003**.

[58] D. Cremer, K. J. Szabo, *Methods in Stereochemical Analysis, Conformational Behavior of Six-Membered Rings, Analysis, Dynamics, and Stereoelectronic Effects* (Ed.: E. Juaristi), VCH, **1995**, 59.

[59] a) K. C. Nicolaou, G. Zuccarello, Y. Ogawa, E. J. Schweiger, T. Kumazawa, *J. Am. Chem. Soc.* **1988**, *110*, 4866; b) J. P. Snyder, *J. Am. Chem. Soc.* **1989**, *111*, 7630; c) J. P. Snyder, G. E. Tipsword, *J. Am. Chem. Soc.* **1990**, *112*, 4040; d) J. P. Snyder, *J. Am. Chem. Soc.* **1990**, *112*, 5367; e) K. IIda, M. Hirama, *J. Am. Chem. Soc.* **1995**, *117*, 88756.

[60] a) R. J. Hall, N. A. Burton, I. H. Hillier, P. E. Young, *Chem. Phys. Lett.* **1994**, *220*, 129; b) S. Woodcock, D. V. S. Green, M. A. Vincent, I. H. Hillier, M. F. Guest, P. Sherwood, *J. Chem. Soc. Perkin Trans. 2* **1992**, 2151.

[61] K. Elmroth, J. M. Nygren, S. Martensson, I. H. Ismail, O. Hammarsten, *DNA Repair* **2003**, *2*, 363.

[62] J. H. Hoffner, M. J. Schottelius, D. Feichtinger, P. Chen, *J. Am. Chem. Soc.* **1998**, *120*, 376.

[63] a) *CRC Handbook of Chemistry and Physics*, 84th ed., CRC PRESS, Boca Raton, USA, **2003–2004**; b) A. V. Morozov, T. Kortemme, D. Baker, *J. Phys. Chem. B* **2003**, *107*, 2075.

[64] a) M. Liedtke, A. H. Saleck, K. M. T. Yamada, G. Winnewisser, D. Cremer, E. Kraka, A. Dolgner, J. Hahn, S. Dobos, *J. Phys. Chem.* **1993**, *97*, 11204; b) D. Cremer, *J. Chem. Phys.* **1978**, *69*, 4456.

[65] T. van der Wijst, C. Fonseca Guerra, M. Swart, F. M. Bickelhaupt, *Chem. Phys. Lett.* **2006**, *426*, 415.

[66] a) J. F. DiJoseph, D. C. Armellino, E. R. Boghaert, K. Khandke, M. M. Dougher, L. Sridharan, A. Kunz, P. R. Hamann, B. Gorovits, C. Udata, J. K. Moran, A. G. Popplewell, S. Stephens, P. Frost, N. K. Damle, *Blood* **2004**, *105*, 1807; b) J. F. DiJoseph, M. E. Goad, M. M. Dougher, E. R. Boghaert, N. K. Damle, E. Bayever, *Blood* **2003**, *102*, 2382; c) A. Prokop, W. Wrasidlo, H. Lode, R. Herold, F. Lang, G. Henze, B. Dorken, T. Wieder, P. T. Daniel, *Oncogene* **2003**, *22*, 9107; d) E. L. Sievers, F. R. Appelbaum, R. T. Speilberger, S. J. Forman, D. Flowers, F. O. Smith, K. Shannon-Dorcy, M. S. Berger, *Blood* **1999**, *93*, 3689.

Received: April 2, 2007
Published online: August 10, 2007

